frontiers | Frontiers in Marine Science

TYPE Original Research
PUBLISHED 04 January 2024
DOI 10.3389/fmars.2023.1319875

OPEN ACCESS

EDITED BY
Michael Yu Roleda,
University of the Philippines Diliman, Philippines

REVIEWED BY
Rita B. Domingues,
University of Algarve, Portugal
Daffne Celeste Lopez Sandoval,
King Abdullah University of Science and Technology, Saudi Arabia
Maxim Gorbunov,
Rutgers, The State University of New Jersey, United States

*CORRESPONDENCE
Joaquin Ortiz
joaquin_ortiz@web.de

RECEIVED 11 October 2023
ACCEPTED 06 December 2023
PUBLISHED 04 January 2024

CITATION
Ortiz J, Arístegui J, Goldenberg SU, Fernández-Méndez M, Taucher J, Archer SD, Baumann M and Riebesell U (2024) Phytoplankton physiology and functional traits under artificial upwelling with varying Si:N.
Front. Mar. Sci. 10:1319875.
doi: 10.3389/fmars.2023.1319875

Phytoplankton physiology and functional traits under artificial upwelling with varying Si:N

Joaquin Ortiz[1,2]*, Javier Arístegui[2], Silvan Urs Goldenberg[1], Mar Fernández-Méndez[3], Jan Taucher[1], Stephen D. Archer[4], Moritz Baumann[1] and Ulf Riebesell[1]

[1]Marine Biogeochemistry, Biological Oceanography, GEOMAR Helmholtz Centre for Ocean Research, Kiel, Germany, [2]Oceanografía Biológica, Instituto de Oceanografía y Cambio Global (IOCAG), Universidad de Las Palmas de Gran Canaria, Las Palmas de Gran Canaria, Spain, [3]Polar Biological Oceanography Section, Alfred Wegener Institute Helmholtz Centre for Polar and Marine Research, Bremerhaven, Germany, [4]Bigelow Laboratory for Ocean Sciences, East Boothbay, ME, United States

Introduction: Artificial upwelling has been discussed as a nature-based solution to fertilize currently unproductive areas of the ocean to enhance food web productivity and atmospheric CO_2 sequestration. The efficacy of this approach may be closely tied to the nutrient stoichiometry of the upwelled water, as Si-rich upwelling should benefit the growth of diatoms, who are key players for primary production, carbon export and food web efficiency.

Methods: With a mesocosm experiment in subtropical waters, we assessed the physiological and functional responses of an oligotrophic phytoplankton community to artificial upwelling under varying Si:N ratios (0.07-1.33).

Results: Deep water fertilization led to strongly enhanced primary productivity rates and net autotrophy across Si scenarios. At the community level, Si-rich upwelling50 temporarily increased primary production and consistently enhanced diatom growth, producing up to 10-fold higher abundances compared to Si-deficient upwelling. At the organism level, contrasting effects were observed. On the one hand, silicification and size of diatom cells remained unaffected by Si:N, which is surprising given the direct dependency of these traits on Si. On the other hand, diatom Chlorophyll *a* density and carbon density were strongly reduced and particulate matter C:N was elevated under Si-rich upwelling.

Discussion: This suggests a reduced nutritional value for higher trophic levels under high Si:N ratios. Despite these strong qualitative changes under high Si, diatom cells appeared healthy and showed high photosynthetic efficiency. Our findings reveal great physiological plasticity and adaptability in phytoplankton under artificial upwelling, with Si-dependent trade-offs between primary producer quantity and quality.

KEYWORDS

primary production, net community production, phytoplankton, stoichiometry, trophic transfer, carbon export, carbon dioxide removal, diatom

1 Introduction

Natural upwelling areas such as eastern boundary upwelling systems provide an abundant and constant supply of nutrients to surface waters, enabling highly productive ecosystems that deliver a large share of the worlds fishery yield (Pauly and Christensen, 1995). This high productivity is attributed to a short food web with high trophic transfer efficiency sustained by the supply of nutrient-rich deep water (Sommer et al., 2002). Consequently, the question has been raised whether upwelling could be artificially induced in oligotrophic, unproductive areas of the ocean as a nature-based technology to sustainably increase fishery yields and enhance the oceans' carbon sequestration capacity. For the former, this depends on the close coupling of primary production to higher trophic levels so that loss of biomass through low trophic transfer efficiency is maximally reduced (Henson et al., 2019). For the latter, producing large amounts of fast sinking carbon-rich biomass is essential so that a large portion of organic carbon reaches sequestration depths and excess upwelled inorganic carbon is compensated for via high C:N ratios.

In oligotrophic systems, nutrients are locked in deeper waters due to stratification. Depending on the remineralization stoichiometry of the sinking matter and the water mass composition of the water column, bringing water from different depths could lead to different nutrient concentrations and ratios. For example, south of the Canary Islands Si:N ratios approximate 0.3-0.5 at 300m, 0.6-0.7 at 1000m and ≥1 beyond 1500m (Schlitzer, 2022). Therefore, depending on the depth of upwelled water, the nutrient composition might differ supporting a different phytoplankton community in the sun-lit surface.

Diatoms play a central role in artificial upwelling, since they are major players in global primary production, strong contributors to carbon export due to their ballasting silica frustules, and a crucial link in short food webs of efficient trophic transfer (Tréguer et al., 2018). As such, supporting a large community of diatoms seems central to both objectives of artificial upwelling. Diatom proliferation largely depends on silicic acid availability as well as its ratio to other macronutrients such as nitrogen (N). In theory, diatoms thrive best under absolute Si concentrations >2 µM (Egge and Aksnes, 1992), with uptake rates that follow Michaelis-Menten kinetics and mostly reach half-saturation at <2 µM (Finkel et al., 2010). The degree of silicification however, can increase with availability up to Si concentrations far beyond those of the current surface ocean. Under N exhaustion, increases in particulate C:N ratios due to diatom carbon overconsumption have been observed (Gilpin et al., 2004).

Recent studies on the effect of a single deep water pulse versus a recurring deep water supply have demonstrated that artificial upwelling leads to strongly increased primary production, biomass and particulate organic carbon export as well as primary producer communities dominated by diatoms regardless of the upwelling mode (Baumann et al., 2021; Ortiz et al., 2022a; Ortiz et al., 2022b). These effects scale with upwelling intensity but are influenced differently by the mode of deep water supply. Recurring deep water supply sustains higher autotrophic biomass and a net autotrophic system whereas a singular pulse leads to a long-term balanced or net heterotrophic community as well as stronger increases in particulate matter C:N ratios.

However, the role of silicic acid in ocean biomass production is still not clear. And information regarding the optimal nutrient composition of upwelled water to achieve the different ecosystem services proposed is scarce. Understanding how phytoplankton physiology and stoichiometry change when growing under different nutrient regimes of the upwelled water will help define the depth of the upwelling pipes in different oceanic locations as well. It is also needed to improve biogeochemical models applied to artificial upwelling (Oschlies et al., 2010), which so far assume constant phytoplankton communities, non-flexible C:N ratios and do no account for the role of Si as a nutrient. Only then can the potential of this approach for carbon dioxide removal and enhanced fisheries be represented accurately.

Building on a previous experiment simulating artificial upwelling in natural oligotrophic plankton communities in the Canary islands (Baumann et al., 2021; Ortiz et al., 2022a; Ortiz et al., 2022b), we set out to explore the impacts of nutrient stoichiometry, specifically the Si:N ratio, on phytoplankton diversity, physiology and organic matter composition under artificial upwelling. For this, we conducted a 33-day long mesocosm study in the subtropical oligotrophic waters of the Canary region. Artificial upwelling was simulated through the recurring supply of deep water with fixed inorganic macro-nutrient concentrations and superimposed Si:N ratios ranging from strongly limiting to abundant from a diatom growth perspective. Community-wide and organism-level effects were assessed via phytoplankton abundance, community composition, metabolic rates, photosynthetic efficiency, morphology, and nutrient utilization. High Si:N upwelling was hypothesized to enhance not only the abundance and dominance of diatoms, but also the presence of large and heavily silicified species supported by excess silicic acid in addition to the abundant supply of nutrients. Yet, the observed response was more multifaceted than expected. We discuss underlying mechanisms that might have modulated some of the surprising outcomes as well as the partly contrasting implications for food web enhancement and carbon export under artificial upwelling.

2 Materials and methods

Details on the experimental setup and the environmental conditions during this experiment are described in Goldenberg et al. (2022). Biogenic silica concentration (BSi) and total particulate matter carbon and nitrogen content are covered therein but are also used as supporting data in this manuscript.

2.1 Mesocosm setup, deep water additions and sampling

During September and October of 2019, eight mesocosms, consisting of large polyurethane bags with a mean volume of 8.29 ± 0.07 m^3 were deployed on the east coast of Gran Canary Island for

a total of 35 experimental days. Total mesocosm length was 4 m including a cone-shaped sediment trap at the bottom. In regular intervals mesocosms were cleaned from the inside and outside to prevent wall growth.

Deep water for upwelling simulation was collected three times by ship from ~120-160 m depth at two different locations (27° 52'16" N, 15° 18'48" W and 28°00'01"N, 15°20'11"W). The deep water was pumped into 1 m^3 food grade plastic containers (IBC tanks) which were then stored in a cooled container at 7°C until use. Every other day, starting on day six, 4% of the mesocosm water volume was replaced by deep water in all treatments. Additionally, a total of 36 larvae and 45 juveniles of the species *Atherina presbyter* were introduced to each mesocosm on day 15.

Each mesocosm received the same amount of deep water with the same nitrate concentration with each addition, but with a different Si:N ratio to represent upwelling of waters of different depths with Si concentrations ranging from excess to strong limitation. The gradient can also be expressed through the absolute difference between Si and N in the deep water ($Si^* = [Si_{Conc}] - [N_{Conc}]$, Sarmiento et al., 2004) with an Si* of 0 indicating equal amounts of Si and N. Nutrient amendments were performed to the collected deep water right before addition to reach 30 µmol L^{-1} N, and phosphate and dissolved inorganic carbon at Redfield ratios (1.9 µmol L^{-1} P, 199 µmol L^{-1} C). Silicic acid (added as $Na_2SiO_3*5H_2O$) was added directly with the deep water in the amounts required for the gradient. The upwelling treatment (continuous addition of nutrients) was developed in accordance with findings from a previous mesocosm study in the same region and season, where we studied the response of the phytoplankton community to different modes of artificial upwelling (Ortiz et al., 2022b). Recurring supply of deep water was found to better sustain a productive and net autotrophic community. In the present study, this upwelling mode was thus successfully applied as the backbone on which the individual Si stoichiometry was imposed.

For water sampling, 2.3 m long plastic sampling tubes with ball valves on both ends were vertically submerged into the mesocosm, closed, and pulled out again, hereby sampling ~5 L of depth-integrated mesocosm water. The tubes were then shaken gently to mix the sample before being emptied into canisters from which each parameter was subsampled.

2.2 Community composition: microscopy, cytometry, and pigment analysis

Phytoplankton taxonomic composition and abundance was assessed using light microcopy. Samples were fixed using Lugol"s and then analyzed according to (Utermöhl, 1931) on a stereomicroscope (Zeiss Axiovert 100, Carl Zeiss, Germany). Species bigger than 5 µm were identified and counted. Taxonomy and abundance were used to compute the Shannon diversity index (H) for diatoms. Size measurements were performed on 3-10 individuals of the most abundant species and the average was used to calculate species-specific biovolumes (Hillebrand et al., 1999; Olenina et al., 2006). If no size measurements were available, the average value from the literature for that species was used.

Additionally, to quantify different phytoplankton size clusters, a Cytosense flow cytometer (CytoBuoy, Woerden, Netherlands) was used in two different settings optimized for small and large taxa: Settings for small taxa had a higher sensitivity (red fluorescence trigger = 10 mV) but lower flow rate, settings for large taxa the other way around (red fluorescence trigger = 18 mV). Sample volume was between 0.5-2 ml for small and large settings respectively. Clusters were identified based on fluorescence profiles, forward scatter (FWS) and side scatter (SWS). FWS signal length was in good accordance with size measurements of particle pictures and was thus chosen as the measure for cell size. To note, the presented size ranges deviate from the canonical 0.2-2 µm, 2-20 µm and >20 µm for pico-, nano- and microphytoplankton due to the size range limit and settings of the device and should be considered an approximation. We grouped the different populations into clusters of approximately <10 µm, 10-40 µm and >40 µm in size. The broad range of 10-40 µm was chosen because the observed phytoplankton bloom emerged over a continuous size range, so that populations would have been artificially split in two if the canonical size ranges were applied as separators. Specific population plots can be found in the Supplementary Material (Supplementary Figure 1).

Samples for photosynthetic pigment analysis were taken and processed as described in (Ortiz et al., 2022b). Pigment-based phytoplankton community composition was estimated using Chemtax v.1.95 based on Higgins et al. (2011, RMS = 0.024).

2.3 Primary productivity & photosynthetic physiology characterization

Oxygen production as well as respiration rates were measured as described in (Ortiz et al., 2022b) using the Winkler titration method and a Dissolved Oxygen Analyzer (SIS Schwentinental, Germany). For each treatment, four replicates of initial oxygen concentrations, "dark" and "light" incubations were measured respectively. All samples were incubated in an outdoor pool with constant seawater flow and "light" samples exposed to ambient day and night cycles. Light samples were randomly distributed inside clear acrylic boxes covered with one layer of blue foil to mimic the light spectrum of the water column inside the mesocosms (172 Lagoon Blue foil, Lee filters, Burbank, USA). Daily light irradiance received by the light incubations ranged from 0.2 to 2141 µmol photons m^{-2} s^{-1} throughout the experiment as measured by light sensor-equipped data loggers inside the incubators (HOBO UA-002-64, Australia/New Zealand). The mean of each fourfold measurement was used for determining the rates for community respiration (CR, Equation 1), net community production (NCP, Equation 2) and gross production (GP, Equation 3) as follows:

$$CR\ [\mu mol\ L^{-1}h^{-1}] = \frac{Conc_I - Conc_D}{h_D} \quad (1)$$

$$NCP\ [\mu mol\ L^{-1}h^{-1}] = \frac{Conc_L - Conc_I}{h_L} \quad (2)$$

$$GP\ [\mu mol\ L^{-1}h^{-1}] = CR + NCP \quad (3)$$

$Conc_I/Conc_D/Conc_L$ = mean oxygen concentration of the Initial/Dark/Light samples; h_D/h_L = hours of incubation of Dark/Light samples. Hourly rates were multiplied by 24 to yield daily rates.

It is worth noting that peak primary productivity rates might have been missed due to the experimental procedure: deep water additions took place on non-sampling days, while incubations for primary productivity measurements did not start until the following sampling day and then ran for another day in enclosed bottles. If nutrients were consumed too quickly the samples might have already been somewhat nutrient limited before the start of the 24h incubations, leading to underestimated NCP.

For photosynthetic physiology characterization, samples of approximately 15 ml were kept in the dark for a minimum of 30 min prior to FRRf measurements, in order to relax non-photochemical processes. Measurements were carried out using a FastOcean FRRf linked to a FastAct module (Chelsea Technologies Group Ltd, UK) allowing discrete fluorescence measurements in the laboratory at *in situ* temperatures. For each sample, approximately 5 ml subsamples were exposed to a single turnover saturation program consisting of 100 x 1 µs excitation flashlets on a 2 µs pitch, followed by 40 x 1 µs relaxation flashlets on a 50 µs pitch. Each acquisition consisted of 40 sequences with an interval of 150 ms between sequences. Over the course of the experiment, excitation flashlets ranged between 1.00 to 1.30 x 10^{22} photons m^{-2} s^{-1} of blue (centred at 450 nm) light. FastPro8 software (Chelsea Technologies) was used to process the data using the biophysical model of (Kolber et al., 1998). The background fluorescence, attributed to the instrument noise and fluorescent dissolved organic matter, was measured in 0.2 µm-filtered seawater on each sampling date and subtracted from the fluorescence data using the FastPro8 software.

2.4 Estimate of diatom carbon density

Estimates of overall phytoplankton or taxon specific biomass are typically calculated applying conversion factors to measured Chl*a* (Sathyendranath et al., 2009) or biovolume (Menden-Deuer and Lessard, 2000) and are widely acknowledged to be highly uncertain (Leblanc et al., 2012). Considering the physiological alterations observed within the diatom community in our study, this approach was also not helpful. Taking the fraction of Chl*a* attributable to diatoms through pigment ratio analysis and converting it to carbon units using fixed diatom- specific Chl*a*:C conversion factors throughout the experimental period would by default ignore any treatment induced temporal changes in actual carbon density. The same applies when calculating biovolume from abundances and converting it to carbon units.

To approximate diatom C, carbon biomass measurements and/or estimates of all organisms other than diatoms were subtracted from the measured total particulate organic carbon (POC) (Equation 4). Heterotroph C biomass included micro- and mesozooplankton (S. Goldenberg, personal correspondence). Under the assumption that non-diatom phytoplankton was not or much less affected by Si:N all Chl*a* attributable to non-diatoms via pigment analysis was pooled and converted to carbon units using a Chl*a*:C quotient of 108.4, which represents the mean Chl*a*:C of all non-diatom groups, including mixotrophs, as measured by Sathyendranath et al. (2009). Taking a mean value of different quotients was the least speculative approach, as Chl*a*:C ratios can vary substantially not only between species but also between oligotrophic and eutrophic systems and numerous other variables (Graff et al., 2015). This non-diatom autotroph carbon biomass was then also subtracted from POC and the resulting value subsequently normalized to diatom abundances, yielding the estimate of diatom carbon density per cell. The time frame (day 15-33) was chosen to exclude the initial burst in productivity following treatment onset and thus better capture the dynamics on the community vs organism level once the system was in a more balanced state.

$$C\ content_{diatom}[pg\ \ C\ \ cell^{-1}] = \quad (4)$$

$$\frac{POC\ \ -B_{heterotroph} - B_{non-diatom\ \ autotroph}[pg\ \ C\ \ L^{-1}]}{abundance_{diatom}\ \ [cells\ \ L^{-1}]}$$

2.5 Internal nutrient storage

Internal nutrient storage (INS; Si, N, P) of cells was measured every 4 days following Dortch (1982) and Dortch et al. (1984). For this, 0.5-1 L of water from the sampling tubes was filtered through 0.2 µm polycarbonate membrane filters (47 mm, GTTP) under low vacuum pressure (200 mbar) to collect all the cells. The filtrate was discarded. Subsequently the Erlenmeyer flask collecting the filtrate was rinsed twice with MilliQ water before being attached to the filter holder again without removing the filter. 40 mL of boiling MiliQ water were poured on the filter and left for 10 minutes for the cells to burst. The filtration pump was turned on again and 10 mL of filtrate were collected in a nutrient sampling tube for photometric measurement along with the water column nutrient samples (Hansen and Koroleff, 1999). A blank consisting of filtered boiling water using the same setup was run every time INS samples were taken.

2.6 Suspended organic matter

For water column particulate organic matter (C, N, P) and biogenic silica (BSi), water samples were filtered under low vacuum pressure. Filters were analyzed as described in (Goldenberg et al., 2022).

2.7 Data analysis

To investigate the general Si:N effect and its temporal development, we applied a linear mixed model (restricted maximum likelihood fit, type III test, Kenward-Roger approximation). Si:N was employed as continuous explanatory variable, mesocosms as random effect and the interaction of Si:N

and day (Si:N x Day) as a factor of the repeated measure design. The factor Day contains various potential sources, such as the upwelling of all other nutrients apart from silicate, enclosure effects and environmental conditions, though the latter did not have a significant impact on the experimental conditions and parameters (Goldenberg et al., 2022).

In addition, a simple linear regression analysis was performed for each sampling day with Si:N as explanatory variable. The slope of each regression ± the 95% confidence interval was then plotted to show the effect size on each day along with the temporal development.

The experiment was also divided into an initial response phase (I, day 8-22) and a longer-term response phase (II, day 22-33) to disentangle the more immediate effects from those that persisted throughout the experimental period. These phases were additionally analyzed through individual linear regression analyses of the phase-averaged response variable.

Finally, to make the effect size of different parameters comparable, the individual phase regression analyses were run again with standardized response variables. Each variable was standardized to a z-score by subtracting from it its sample mean and then dividing it by its standard deviation. From these transformed phase regressions, we extracted the slope and standard error for a comparative analysis. All data analyses were performed with R (R Core Team, 2022; Posit team, 2023). Data were checked for deviations from normality using Q-Q plots and homogeneity of variance with residual versus fitted plots.

3 Results

3.1 Community functionality and composition

During the initial response phase, the central ecosystem function of primary productivity responded in the form of a temporary positive Si:N effect on GP, photosynthetic electron transport rate, *in situ* oxygen concentration and CR in the face of equal N and P supply (Figures 1A–C; Supplementary Figure 3). The increase in oxygen concentration was driven by a 5-fold increase in GP. In the longer-term response however, this effect dissipated in all three parameters despite the 20-fold difference in Si loading between the lowest and highest treatment. In general, deep-water upwelling succeeded in sustaining a net autotrophic community (Supplementary Figure 1A, Goldenberg et al., 2022).

The nutrient input from artificial upwelling drove the size distribution toward large phytoplankton (Figures 1D, E bottom). In addition, increasing Si availability significantly favored large phytoplankton (Figures 1D, E). This positive Si:N effect was present throughout both experimental phases and culminated in an 11 and 5-fold difference in abundances between the highest and lowest Si:N in the >40 µm and 10-40 µm clusters respectively (day 33). Small phytoplankton abundance, on the other hand, benefited from Si deficiency (negative Si:N effect) in phase I, but this effect dissipated in phase II (Figure 1F).

Overall, the transient positive Si:N effect on primary productivity and community metabolism developed on top of the ubiquitously elevated productivity and the persistent positive effects on large phytoplankton abundances. This Si:N-driven surplus in growth despite similar primary productivity rates across treatments in the longer-term implies that phytoplankton functionality must have been altered along the Si:N gradient.

3.2 Diatom performance

Upwelled Si:N increased diatom abundances throughout both phases, which was mirrored by the strong positive effect on biogenic silica (Supplementary Figure 4C). This resulted in an almost 10-fold larger diatom community after 27 days of treatment (Figure 2A), with diatoms quickly outnumbering other phytoplankton classes (Figure 2B). This was contrasted by only a brief positive Si:N effect on diatom contribution to total Chl*a* (Figure 2C) in the initial phase, indicating that changes within the diatom community must have occurred. At Si:N ≤1 non-diatom phytoplankton concentrations remained relevant during the initial phase, and throughout both phases under Si:N 0.07 (Figure 2B).

Contrary to the initial hypothesis, neither cell size of diatoms nor per cell silicification were enhanced under increasing Si availability, as revealed by the absence of an Si:N effect in both phases (Figures 3A, B). This confirms that both the dominance of diatoms over other phytoplankton as well as the pronounced treatment effect on concentrations of biogenic silica were essentially driven by the increase in cell numbers and not by morphological changes.

On a physiological level, intracellular Si storage increased with increasing Si:N with the effect becoming stronger in phase II (Figure 3C). Which indicates that excess silicic acid was stored inorganically instead of being used to develop thicker frustules. This aligns with decreasing residual silicic acid in the mesocosms as the experiment evolved (Supplementary Figure 2, Goldenberg et al., 2022). Both points suggest that the enclosed communities were not limited by Si. Rather, periodic N-limitation likely occurred in the short periods between nutrient consumption and the following deep water addition, with P becoming co-limiting from day 15 onwards (Supplementary Figure 2).

In contrast, light harvesting capacity in terms of per cell Chl*a* was about 2.5-fold higher under scarce than under abundant Si throughout both response phases (Figure 3D). This indicates that per cell Chl*a* content of the phytoplankton community, was strongly reduced under high Si:N. This was not a consequence of e.g., cellular stress or changing light conditions, since photosynthetic efficiency increased slightly with Si:N (Figure 3E). Electron transport rates also increased consistently at least until day 27, implying that phytoplankton (and thus diatom) physiology was

10.3389/fmars.2023.1319875

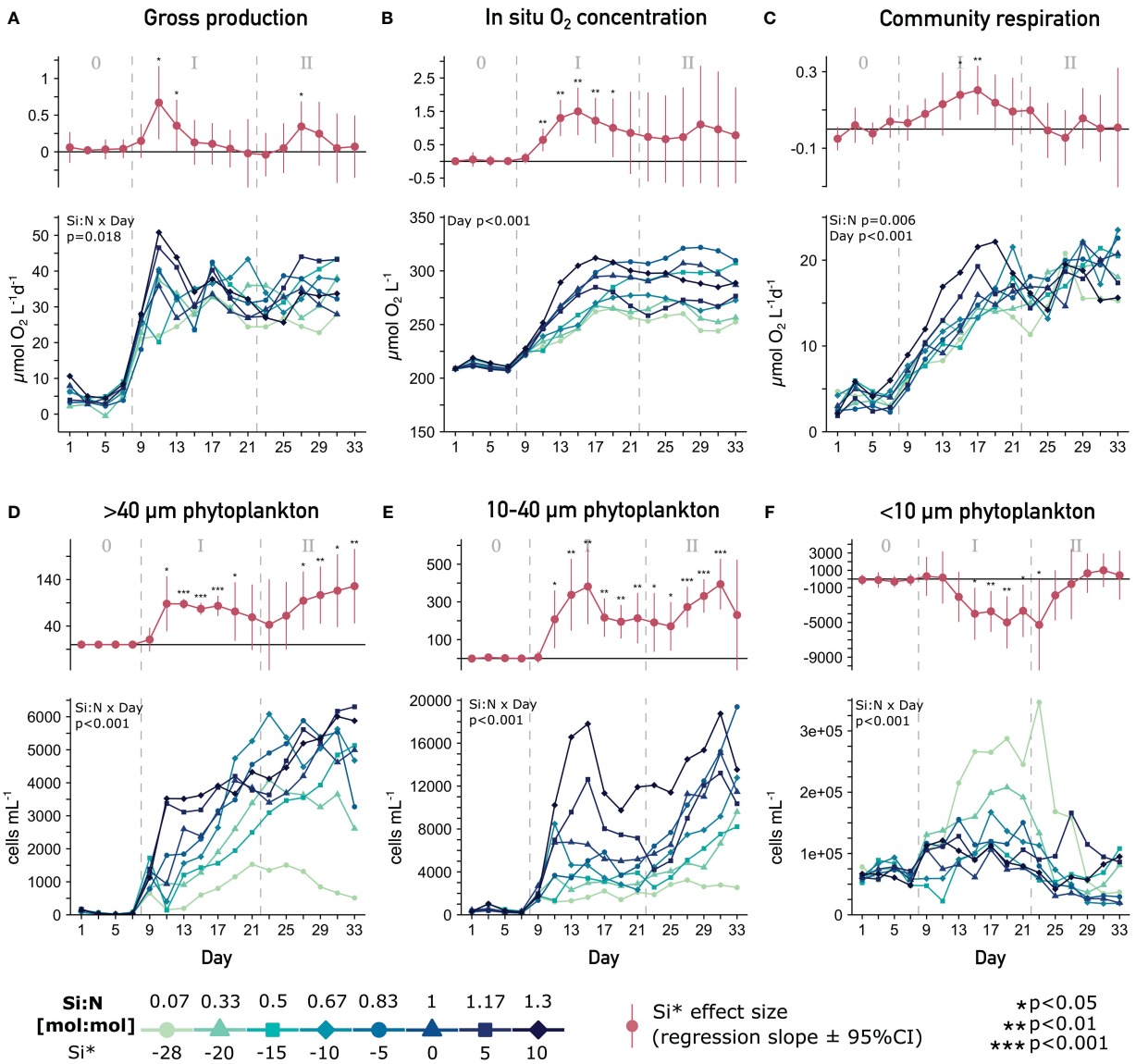

FIGURE 1
Phytoplankton community metabolism and composition under varying Si:N upwelling. Top parts of each plot show the Si:N effect size (slope ± 95% confidence interval of the linear regression for that day (red lines)). Bottom parts show the temporal development of **(A)** gross production, **(B)** *in situ* oxygen concentration, **(C)** community respiration and phytoplankton abundances in the **(D)** >40 µm, **(E)** 10-40 µm and **(F)** <10 µm size range clusters. Significant effects of the mixed model across time (Si:N, Day, Si:N x Day) provided in top left corners. 0/I/II = oligotrophic baseline/short-term/long-term response phase.

altered, but not impaired despite the wide range of Si:N (Supplementary Figure 3). Also, while light intensity varied from day to day, there was no progressive change over time due to the developing phytoplankton blooms (Goldenberg et al., 2022).

Our approach to estimate changes in diatom carbon density over time (see section 2.6) revealed that the larger diatom communities sustained under higher Si:N upwelling contained notably less carbon, as opposed to small communities under low Si:N upwelling (Figure 3F).

In contrast to the positive community-wide effects, morphological diatom properties on the individual level (size & silicification) did not scale with Si availability. Photosynthetic efficiency was unconstrained and slightly higher with increasing Si:N, whereas other physiological properties like per cell Chl*a* and carbon density persistently decreased with increasing Si:N.

4 Discussion

Our study demonstrates how the manipulation of Si:N ratios shapes the response of phytoplankton exposed to nutrient-rich deep water upwelling in contrasting ways.

On the community level, high Si:N upwelling led to higher abundances and a diatom-dominated phytoplankton community with higher absolute amounts of ballasting BSi and, initially, also higher energy input to the system via primary production

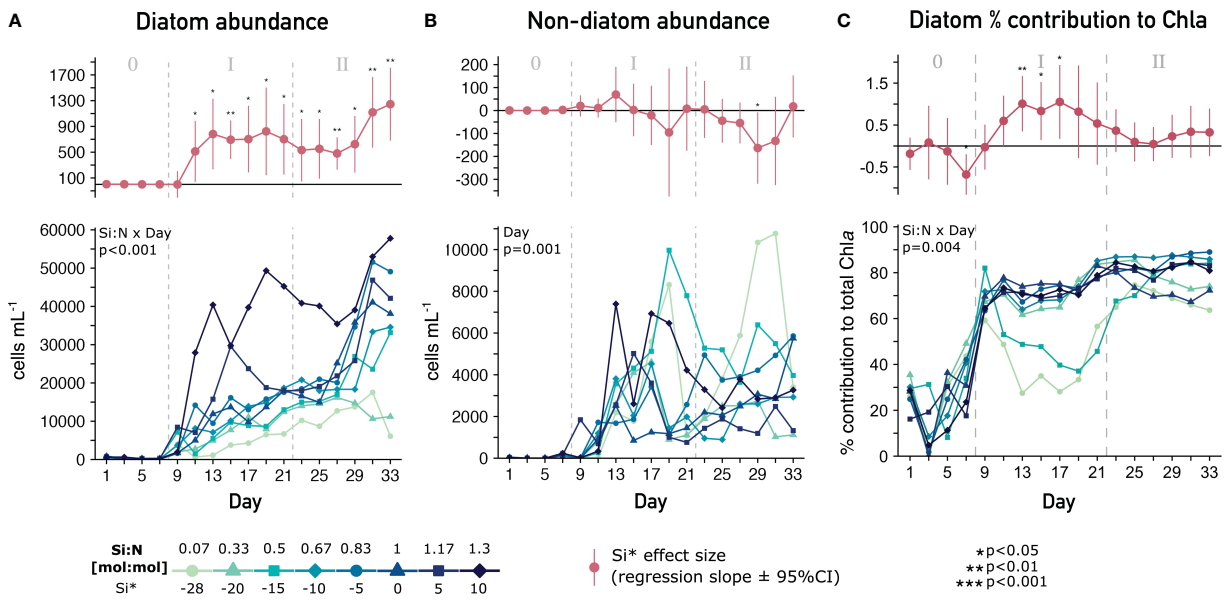

FIGURE 2
Quantitative diatom performance under varying Si:N upwelling. Top parts of each plot show the Si:N effect size (slope ± 95% confidence interval of the linear regression for that day (red lines)). Bottom parts show the temporal development of **(A)** diatom abundance **(B)** on-diatom abundance assessed through microscopy and **(C)** relative diatom contribution to total Chl*a* assessed through pigment analysis (Chemtax). Significant effects of the mixed model across time (Si:N, Day, Si:N x Day) provided in top left corners. 0/I/II = oligotrophic baseline/short-term/long-term response phase.

(Figure 4A). High Si:N ratios also temporarily increased suspended organic carbon concentrations and particulate matter C:N ratios, indicating enhanced carbon sequestration. The latter remained beyond Redfield ratios throughout the experiment (Supplementary Figure 1G).

On the organism level, high Si availability did not promote the growth of larger or more heavily armored diatoms as hypothesized but led to strongly reduced per cell Chl*a* and carbon density. Thus, differences in Si:N led to a stark differentiation between a large population size of reduced organism quality for grazers under high Si:N versus a smaller, comparatively more palatable community under low Si:N (Figure 4B). In the following sections, we discuss these developments step-by-step and deliberate on the potential implications for trophic transfer and carbon export under artificial upwelling.

4.1 Phytoplankton physiological and community response

The positive correlation between Si:N and the abundance of diatoms and phytoplankton overall was among the strongest observed community-wide effects in our study. This would suggest that Si availability set the upper boundary for population growth. However, small quantities of leftover Si as well as increasing internal Si storage indicate that N was the first macronutrient to become limiting (Supplementary Figure 2). In fact, both N and P were consumed increasingly fast after each addition, with N reaching detection limits within 24 hours in almost all treatments. The ability of diatoms to modulate Si uptake and their degree of silicification in adaptation to shifting nutrient limitations provides a mechanistic explanation for this (Martin-Jézéquel et al., 2000; McNair et al., 2018). The transient positive Si:N effect on primary production likely signaled the alleviation of Si limitation after treatment onset, and before the community adjusted its uptake speed to the N and P supply. On a similar note, the brief Si:N-mediated increase in electron transport rates (Supplementary Figure 3) might also hint toward a diatom sub-population that responded even quicker than others to the treatment onset.

The subsequent diminishing of the primary productivity response, and the simultaneous emergence of the positive effect on C:N ratios, on the other hand, indicate a potential shift in growth-limiting factors still within the initial phase (Figure 1A, Supplementary Figure 1G). We attribute this to a shift from N- to N & P co-limitation, which is corroborated by steadily increasing concentrations of organic phosphorus from approximately day 15 onwards (Martin et al., 2014; Goldenberg et al., 2022). It might also explain the brief disappearance of the Si:N effect in the largest (>40 µm) phytoplankton fraction. This shift in limitations represents a relevant difference from a physiological point of view since P is critical for reproductive processes such as membrane synthesis and DNA replication, whereas N is also necessary for the synthesis of Chl*a* and amino acids. However, both N- and P-limitation do not affect diatom growth as quickly as Si limitation (Parslow et al., 1984; Harrison et al., 1990). This is due to Si only being stored in soluble pools within the cell, whereas N and P can be salvaged from the breakdown of intracellular material if necessary. Which offers an explanation to why the phytoplankton community was much less dominated by diatoms under Si:N ratios <0.5 in our study. Lastly, a limiting role of micronutrients cannot be excluded, though we do not have corresponding analyses. Particularly iron measurements cannot be performed accurately in the mesocosms due to the

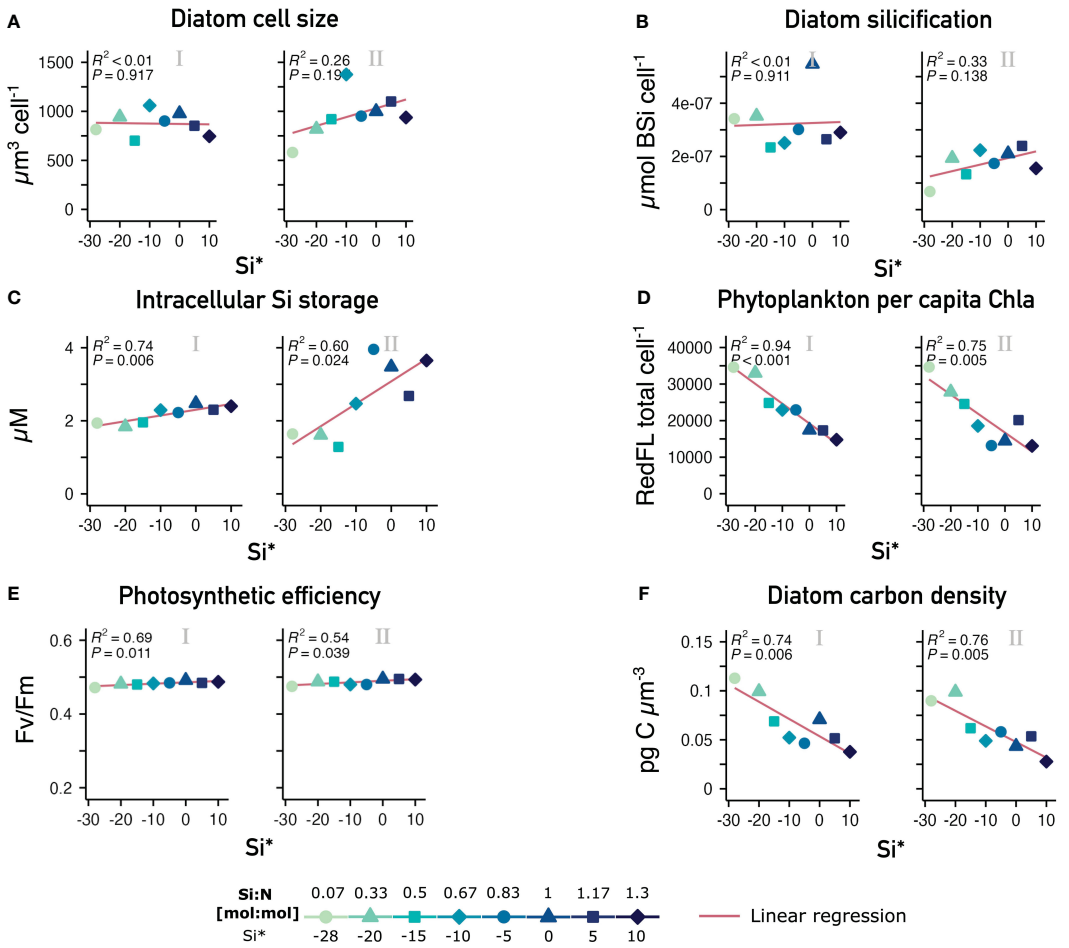

FIGURE 3
Morphological and physiological effects of varying Si:N upwelling on diatoms and phytoplankton overall. Phase-averaged values and linear regressions of **(A)** diatom cell size and **(B)** per cell silicification of diatom cells assessed through microscopy and BSi concentration as well as **(C)** intracellular inorganic Si storage and **(D)** Chl*a* per cell of the large phytoplankton community by proxy of total red FL normalized to abundances in the pooled 10-40 µm and >40µm clusters (flow cytometry). **(E)** shows photosynthetic quantum yield (Fv/Fm) of the whole phytoplankton community and **(F)** the estimate of diatom carbon density. Regression model R^2 and p-values in top left corners. 0/I/II = oligotrophic baseline/short-term/long-term response phase.

presence of metal parts that can alter trace metal concentrations which, however, also render iron limitation highly unlikely (Bach et al., 2020; Baumann et al., 2023).

In terms of photosynthetic capacity and efficiency, it is evident that the favorable conditions created by the nutrient-rich deep water addition and high light availability, sustained a level of autotrophy that did not require Chl*a* content to scale proportionally with abundances to grow. This is manifested in the high degrees of photosynthetic efficiency maintained across all treatments despite a decline in fluorescence per cell under increasing Si:N. On the contrary, high Si availability with an equal supply of N and P, might have further facilitated cell division leading to higher abundances but with reduced per cell Chl*a*. Since N is necessary for Chl*a* synthesis, the reduction of per cell Chl*a* might have been, if anything, another response to the intermittent N-limitation in our study caused by the addition of deep water every 2 days. It is important to note as well, that Fv/Fm has been shown to be a poor indicator of nutrient stress (Gorbunov and Falkowski, 2021), so that the persistently stable photosynthetic efficiency values observed throughout the experiment might have obscured any periods of nutrient limitation.

A mechanistic rationalization for the sustained high photosynthetic efficiency can moreover be found on the organism level: The subtle increase in photosynthetic efficiency observed under increasing Si:N can be explained by the matching increase in diatom abundance, as their frustules have been shown to enhance light absorption efficiency (Romann et al., 2015). Inversely, this might also explain why the magnitude of the drop in electron transport rates during the last 6 days was larger in the low Si:N treatments, as these had a less diatom dominated community (Supplementary Figure 3).

Among the rather surprising findings on the organism level were the absence of any changes in diatom cell size and per cell silicification, as both were expected to increase along with Si:N (Figure 4A). Nutrient inputs to an oligotrophic phytoplankton community typically trigger a succession not only toward higher diatom abundance, but also toward larger cell sizes and diatom species (McAndrew et al., 2007; Fawcett and Ward, 2011). In our

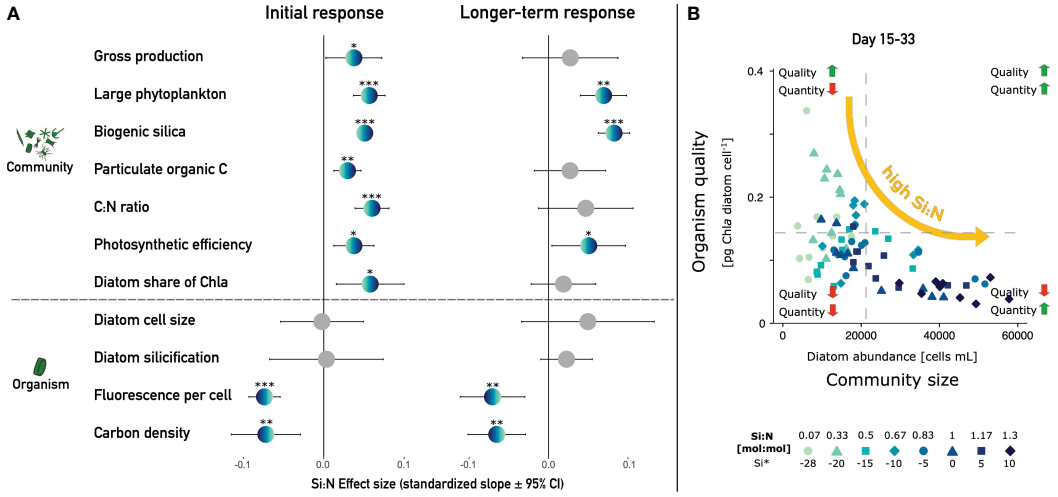

FIGURE 4
Contrasting effects of Si:N on the community and organism level. **(A)** Standardized effect sizes during both experimental phases. Large phytoplankton refers to abundances in the combined 10-40 & >40 µm cytometry clusters. Significant effects (Slope ± 95% CI does not cross 0) are in color and significance levels are denoted (*/**/*** equals p < 0.05/0.01/0.001). **(B)** Trade-off between diatom quantity and quality exemplified via diatom abundance (x-axis) versus per cell Chla content of diatoms (y-axis).

study, the shift toward larger phytoplankton and diatoms was observed. But there were no large taxonomic changes as the diatom community was continuously dominated by the two chain-forming genera *Leptocylindrus* & *Pseudo-nitzschia*. Both similar in size and elongated shape, *Pseudo-nitzschia* was more relevant during the short term response and only maintained noteworthy relative abundances at Si:N >1 (Goldenberg et al., 2022). The Si:N dependent increase in large phytoplankton was thus driven by Si availability allowing higher reproduction rates of the same genus rather than selecting toward larger species; and highlights the plasticity and capability of these genera to get the most out of any given Si availability scenario under artificial upwelling. Their elongated shape and the ability to form chains likely represented an additional advantage in terms of nutrient uptake capability and grazer protection (Pahlow et al., 1997).

The lack of any effect on per cell silicification coupled with the much larger diatom population under high Si:N upwelling additionally confirms that diatoms capitalized on the available Si via reproduction rather than investing energy in the development of thicker frustules. This is also in line with studies showing a reduction in duration of the cell wall synthesis phase under high growth rates (Martin-Jézéquel et al., 2000 and references therein). Grazing pressure can trigger thicker frustule development or select toward more heavily armored species, but was not a dominant driver during our study (Grønning and Kiørboe, 2020; Ryderheim et al., 2022). This can partly be attributed to the introduction of the fish larvae on day 15, which evenly decimated the zooplankton community that was responding to the phytoplankton bloom across all treatments (S. Goldenberg, pers. comm.). Consequently, we cannot fully confirm that the reduced quality of diatoms translated into reduced zooplankton growth. Yet there was also no Si:N effect on per cell silicification in the timeframe between treatment onset and fish introduction (day 6-15, Supplementary Figure 1D). A positive effect could have been expected independently of the grazing situation, considering that frustules provide other benefits such as improved nutrient uptake and light harvesting (Mitchell et al., 2013; Romann et al., 2015). An absence of heavy armoring in the diatom community would certainly benefit the grazer community in terms of prey palatability, at least until the "arms race" of pelagic predator-prey interactions is re-established (Smetacek, 2012).

Lastly, it is worth elaborating on the seemingly contradictory interpretation of both increased particulate matter C:N and reduced diatom carbon density as indicators of reduced quality. Typically, high C:N ratios in phytoplankton are associated with reduced nutritional value for grazers, as they point toward lower relative protein content (Hessen, 1992). Simply put, grazers must consume relatively more unnecessary C to gain the same amount of N (or P for that matter). In our study, Si:N was the main driver of the increase in particulate matter C:N ratios not only in the initial phase (Figure 4A), given that it was still present in form of a curvilinear relationship in phase II (Goldenberg et al., 2022). High Si:N upwelled water consequently reduces phytoplankton quality for grazers via high relative carbon content in the organic matter. The estimate of carbon density on the other hand gauges the amount of carbon per diatom biovolume. A strongly reduced carbon density under high Si:N upwelling thus means that diatom cells in those treatments had less overall carbon content, i.e., that they were less densely packed or "waterier". Therefore, high C:N and low per cell carbon density both indicate that grazers receive less nutritionally valuable components per ingested cell when grazing on these diatoms.

4.2 Potential for food web enhancement

We demonstrated that the reduced N content relative to C as well as waterier diatom cells that develop under constant irrigation

with high Si:N upwelled waters is counterproductive to achieve efficient trophic transfer. This stands in contrast to the general understanding that diatom dominated phytoplankton communities are best to maintain higher trophic levels. Additionally, the dominance of chain forming diatom species could further contribute to this via reduced palatability. It is worth mentioning, however, that our particulate matter C:N ratios included potentially carbon rich detritus on top of all the organisms, which might lead to an overestimation of C:N ratios of live phytoplankton cells.

Inversely, a more heterogeneous phytoplankton community with lower C:N as observed under low Si:N upwelling would promote herbivore growth, as these would profit from more nutritious (albeit less numerous) diatoms and the benefits of a more mixed diet (Schmidt and Jónasdóttir, 1997). Dinoflagellates, for example, are also less susceptible to fluctuations in nutrient availability and could constitute a more reliable food source (Jones et al., 2002). Additionally, a lack of Si does not seem to impact the nutritional value of diatoms (and certainly not that of non-silicifying phytoplankton), whereas N starvation leads to reduced protein content and can thus negatively affect higher trophic levels (Harrison et al., 1990). There is also evidence that even excessive quantities of low quality food cannot support crustacean growth rates comparable to those achieved at low but nutritious phytoplankton densities (Sterner et al., 1993). Lastly, if high-quality diatoms already thrive at lower-than-expected Si:N ratios, Si:N ratios <0.5 in the upwelled water might be enough for the goal of increasing food web productivity.

The absence of an Si:N effect on per cell silicification and the overall shift toward larger phytoplankton do speak in favor of high Si:N upwelling, at least if a classic pelagic food web structure with few trophic levels is maintained (Sommer et al., 2002). However, the status of diatoms as the ideal food source for herbivores is increasingly debated (Ianora and Miralto, 2010). Solely driving the system toward maximum diatom abundance is therefore unlikely to create the best conditions for efficient trophic transfer under artificial upwelling.

4.3 Consequences for carbon export potential

When evaluating our findings from a perspective of increasing carbon export potential through artificial upwelling we can see opposing effects of the Si:N ratio. Here, the same input to the system in terms of nutrients and primary production resulted in presumably better carbon export conditions under high Si:N upwelling: a significantly larger diatom population and more than 20-fold higher final concentration of suspended BSi in the highest treatment (compared to the lowest). Both factors could greatly enhance (carbon) export fluxes via unconstrained diatom growth, and thus particulate matter generation, and ballasting effects of BSi, respectively.

However, while the upwelling of nutrients alone (N & P) already led to a doubling of exported particulate matter and increased the C:N ratio of sedimented material, the Si:N treatment had counteracting effects on the export flux (Baumann et al., 2023). These positive (C export, C:N of exported matter) and negative (particle size & velocity) effects were only present in the initial phase, where the dominance of diatoms was not yet fully established in all treatments. Phytoplankton community composition might thus have been a relevant driver of the altered particle properties observed by the authors. The reduced diatom carbon density under high Si:N might have ultimately also led to the disappearance of the positive Si:N effect on carbon export in the longer term.

Lastly, carbon export fluxes also strongly depend on the repackaging of phytoplankton and particulate organic matter through grazers, whose role was difficult to evaluate in our study due to a strong mismatch between both communities. In essence, the effort of actively providing Si-rich artificial upwelling is unlikely to produce a relevant added benefit for carbon export as compared to lower Si:N upwelling.

5 Conclusions

We examined the effects of artificial upwelling with different Si:N ratios representing different source depths (~300-2000 m) of the upwelled waters, on a natural oligotrophic phytoplankton community in the subtropical North Atlantic. Primary productivity, phytoplankton abundance and biomass were greatly increased under all treatments. Increasing Si availability strongly enhanced diatom community size at the expense of their nutritional value and a more heterogenous phytoplankton community, thus resulting in a quality (low Si:N) versus quantity (high Si:N) trade-off. Our findings consequently suggest that low Si:N upwelling might create better conditions for efficient trophic transfer via better food quality for grazers, while high Si:N upwelling might provide higher carbon export via overall biomass and BSi production. Whether this might render both goals mutually exclusive under a given nutrient signature needs to be investigated. Overall, the diatom community showed a remarkable degree of intraspecific plasticity that allowed it to thrive even at Si:N ratios considered unfavorable and below their own (Brzezinski, 1985; Sarthou et al., 2005). This warrants a more mechanistic evaluation of the conditions required for diatoms to flourish rather than adhering to e.g., nutrient threshold values.

Data availability statement

The datasets presented in this study can be found in online repositories. The names of the repository/repositories and accession number(s) can be found below: PANGAEA: https://doi.pangaea.de/10.1594/PANGAEA.962782.

Author contributions

JO: Formal analysis, Writing – original draft, Writing – review & editing. JA: Supervision, Writing – review & editing. SUG: Writing – review & editing. MF: Writing – review & editing. JT: Writing – review & editing. SA: Writing – review & editing. MB:

Writing – review & editing. UR: Funding acquisition, Supervision, Writing – review & editing.

Funding

The author(s) declare financial support was received for the research, authorship, and/or publication of this article. This project was conducted in the framework of the projects Ocean Artificial Upwelling (Ocean artUp, No. 695094) funded by an Advanced Grant of the European Research Council awarded to UR, and Test-ArtUp funded by the German Marine Research Alliance (DAM) as part of the CDRmare research mission (No. 03F0897B). Additional support was provided through Transnational Access funds by the EU project AQUACOSM, EU H2020-INFRAIA-project (No. 731065).

Acknowledgments

We would like to thank the Plataforma Oceanica de Canarias (PLOCAN) and the Parque Científico Tecnológico Marino (PCTM) for their ongoing support with infrastructure, Acorayda González Pérez for her technical support in the measurements of primary productivity rates, and Madeleine Archer for the FRRf measurements.

Conflict of interest

The authors declare that the research was conducted in the absence of any commercial or financial relationships that could be construed as a potential conflict of interest.

The author(s) declared that they were an editorial board member of Frontiers, at the time of submission. This had no impact on the peer review process and the final decision.

Publisher's note

Supplementary material

The Supplementary Material for this article can be found online at: https://www.frontiersin.org/articles/10.3389/fmars.2023.1319875/full#supplementary-material

References

Bach, L. T., Paul, A. J., Boxhammer, T., von der Esch, E., Graco, M., Schulz, K. G., et al. (2020). Factors controlling plankton community production, export flux, and particulate matter stoichiometry in the coastal upwelling system off Peru. *Biogeosciences* 17, 4831–4852. doi: 10.5194/bg-17-4831-2020

Baumann, M., Goldenberg, S. U., Taucher, J., Fernández-Méndez, M., Ortiz, J., Haussmann, J., et al. (2023). Counteracting effects of nutrient composition (Si:N) on export flux under artificial upwelling. *Front. Mar. Sci.* 10. doi: 10.3389/fmars.2023.1181351

Baumann, M., Taucher, J., Paul, A. J., Heinemann, M., Vanharanta, M., Bach, L. T., et al. (2021). Effect of intensity and mode of artificial upwelling on particle flux and carbon export. *Front. Mar. Sci.* 8. doi: 10.3389/fmars.2021.742142

Brzezinski, M. A. (1985). The Si:C:N ratio of marine diatoms: Interspecific variability and the effect of some environmental variables. *J. Phy* 21, 347–357. doi: 10.1111/j.0022-3646.1985.00347.x

Dortch, Q. (1982). Effect of growth conditions on accumulation of internal nitrate, ammonium, amino acids, and protein in three marine diatoms. *J. Exp. Mar. Biol. Ecol.* 61, 243–264. doi: 10.1016/0022-0981(82)90072-7

Dortch, Q., Clayton, J. R., Thoresen, S. S., and Ahmed, S. I. (1984). Species differences in accumulation of nitrogen pools in phytoplankton. *Mar. Biol.* 81, 237–250. doi: 10.1007/BF00393218

Egge, J., and Aksnes, D. (1992). Silicate as regulating nutrient in phytoplankton competition. *Mar. Ecol. Prog. Ser.* 83, 281–289. doi: 10.3354/meps083281

Fawcett, S. E., and Ward, B. B. (2011). Phytoplankton succession and nitrogen utilization during the development of an upwelling bloom. *Mar. Ecol. Prog. Ser.* 428, 13–31. doi: 10.3354/meps09070

Finkel, Z. V., Matheson, K. A., Regan, K. S., and Irwin, A. J. (2010). Genotypic and phenotypic variation in diatom silicification under paleo-oceanographic conditions: Diatom silicification. *Geobiology* 8, 433–445. doi: 10.1111/j.1472-4669.2010.00250.x

Gilpin, L. C., Davidson, K., and Roberts, E. (2004). The influence of changes in nitrogen: silicon ratios on diatom growth dynamics. *J. Sea Res.* 51, 21–35. doi: 10.1016/j.seares.2003.05.005

Goldenberg, S. U., Taucher, J., Fernández-Méndez, M., Ludwig, A., Arístegui, J., Baumann, M., et al. (2022). Nutrient composition (Si:N) as driver of plankton communities during artificial upwelling. *Front. Mar. Sci.* 9. doi: 10.3389/fmars.2022.1015188

Gorbunov, M. Y., and Falkowski, P. G. (2021). Using chlorophyll fluorescence kinetics to determine photosynthesis in aquatic ecosystems. *Limnol. Oceanography* 66, 1–13. doi: 10.1002/lno.11581

Graff, J. R., Westberry, T. K., Milligan, A. J., Brown, M. B., Dall'Olmo, G., Dongen-Vogels, V. V., et al. (2015). Analytical phytoplankton carbon measurements spanning diverse ecosystems. *Deep Sea Res. Part I.: Oceanographic Res. Papers* 102, 16–25. doi: 10.1016/j.dsr.2015.04.006

Grønning, J., and Kiørboe, T. (2020). Diatom defence: Grazer induction and cost of shell-thickening. *Funct. Ecol.* 34, 1790–1801. doi: 10.1111/1365-2435.13635

Hansen, H. P., and Koroleff, F. (1999). "Determination of nutrients," in *Methods of Seawater Analysis* (Weinheim, Germany: Wiley-VCH), 159–228.

Harrison, P. J., Thompson, P. A., and Calderwood, G. S. (1990). Effects of nutrient and light limitation on the biochemical composition of phytoplankton. *J. Appl. Phycol.* 2, 45–56. doi: 10.1007/BF02179768

Henson, S., Le Moigne, F., and Giering, S. (2019). Drivers of carbon export efficiency in the global ocean. *Global Biogeochem. Cycles* 33, 891–903. doi: 10.1029/2018GB006158

Hessen, D. O. (1992). Nutrient element limitation of zooplankton production. *Am. Nat.* 140, 799–814. doi: 10.1086/285441

Higgins, H., Wright, S., and Schluter, L. (2011). "Quantitative interpretation of chemotaxonomic pigment data," in *Phytoplankton Pigments: Characterization, Chemotaxonomy and Applications in Oceanography* (Cambridge, England: Cambridge University Press), 257–313.

Hillebrand, H., Dürselen, C.-D., Kirschtel, D., Pollingher, U., and Zohary, T. (1999). Biovolume calculation for pelagic and benthic microalgae. *J. Phycol.* 35, 403–424. doi: 10.1046/j.1529-8817.1999.3520403.x

Ianora, A., and Miralto, A. (2010). Toxigenic effects of diatoms on grazers, phytoplankton and other microbes: a review. *Ecotoxicology* 19, 493–511. doi: 10.1007/s10646-009-0434-y

Jones, R., Flynn, K., and Anderson, T. (2002). Effect of food quality on carbon and nitrogen growth efficiency in the copepod Acartia tonsa. *Mar. Ecol. Prog. Ser.* 235, 147–156. doi: 10.3354/meps235147

Kolber, Z. S., Prášil, O., and Falkowski, P. G. (1998). Measurements of variable chlorophyll £uorescence using fast repetition rate techniques: defining methodology

and experimental protocols. *Biochim. Biophys. Acta* 1367, 88–106. doi: 10.1016/S0005-2728(98)00135-2

Leblanc, K., Arístegui, J., Armand, L., Assmy, P., Beker, B., Bode, A., et al. (2012). A global diatom database – abundance, biovolume and biomass in the world ocean. *Earth Syst. Sci. Data* 4, 149–165. doi: 10.5194/essd-4-149-2012

Martin, P., Dyhrman, S. T., Lomas, M. W., Poulton, N. J., and van mooy, B. A. S. (2014). Accumulation and enhanced cycling of polyphosphate by Sargasso Sea plankton in response to low phosphorus. *Proc. Natl. Acad. Sci. U.S.A.* 111, 8089–8094. doi: 10.1073/pnas.1321719111

Martin-Jézéquel, V., Hildebrand, M., and Brzezinski, M. A. (2000). Silicon metabolism in diatoms: implications for growth. *J. Phycol.* 36, 821–840. doi: 10.1046/j.1529-8817.2000.00019.x

McAndrew, P., Björkman, K., Church, M., Morris, P., Jachowski, N., Williams, P. J., et al. (2007). Metabolic response of oligotrophic plankton communities to deep water nutrient enrichment. *Mar. Ecol. Prog. Ser.* 332, 63–75. doi: 10.3354/meps332063

McNair, H. M., Brzezinski, M. A., and Krause, J. W. (2018). Diatom populations in an upwelling environment decrease silica content to avoid growth limitation. *Environ. Microbiol.* 20, 4184–4193. doi: 10.1111/1462-2920.14431

Menden-Deuer, S., and Lessard, E. J. (2000). Carbon to volume relationships for dinoflagellates, diatoms, and other protist plankton. *Limnol. Oceanogr.* 45, 569–579. doi: 10.4319/lo.2000.45.3.0569

Mitchell, J. G., Seuront, L., Doubell, M. J., Losic, D., Voelcker, N. H., Seymour, J., et al. (2013). The role of diatom nanostructures in biasing diffusion to improve uptake in a patchy nutrient environment. *PloS One* 8. doi: 10.1371/journal.pone.0059548

Olenina, I., Hajdu, S., Edler, L., Andersson, A., Wasmund, N., Busch, S., et al. (2006). Biovolumes and size-classes of phytoplankton in the Baltic Sea HELCOM Balt. *Sea Environ. Proc.* 106, 144

Ortiz, J., Arístegui, J., Hernández-Hernández, N., Fernández-Méndez, M., and Riebesell, U. (2022a). Oligotrophic phytoplankton community effectively adjusts to artificial upwelling regardless of intensity, but differently among upwelling modes. *Front. Mar. Sci.* 9. doi: 10.3389/fmars.2022.880550

Ortiz, J., Arístegui, J., Taucher, J., and Riebesell, U. (2022b). Artificial upwelling in singular and recurring mode: consequences for net community production and metabolic balance. *Front. Mar. Sci.* 8. doi: 10.3389/fmars.2021.743105

Oschlies, A., Pahlow, M., Yool, A., and Matear, R. J. (2010). Climate engineering by artificial ocean upwelling: Channelling the sorcerer's apprentice: OCEAN PIPE IMPACTS. *Geophys. Res. Lett.* 37. doi: 10.1029/2009GL041961

Pahlow, M., Riebesell, U., and Wolf-Gladrow, D. A. (1997). Impact of cell shape and chain formation on nutrient acquisition by marine diatoms. *Limnol. Oceanogr.* 42, 1660–1672. doi: 10.4319/lo.1997.42.8.1660

Parslow, J. S., Harrison, P. J., and Thompson, P. A. (1984). Saturated uptake kinetics: transient response of the marine diatom Thalassiosira pseudonana to ammonium, nitrate, silicate or phosphate starvation. *Mar. Biol.* 83, 51–59. doi: 10.1007/BF00393085

Pauly, D., and Christensen, V. (1995). Primary production required to sustain global fisheries. *Nature* 374, 255–257. doi: 10.1038/374255a0

Posit team (2023). *RStudio: Integrated Development Environment for R*. Available at: http://www.posit.co/.

R Core Team (2022). *R: A language and environment for statistical computing*. Available at: https://www.R-project.org/.

Romann, J., Valmalette, J.-C., Chauton, M. S., Tranell, G., Einarsrud, M.-A., and Vadstein, O. (2015). Wavelength and orientation dependent capture of light by diatom frustule nanostructures. *Sci. Rep.* 5, 17403. doi: 10.1038/srep17403

Ryderheim, F., Grønning, J., and Kiørboe, T. (2022). Thicker shells reduce copepod grazing on diatoms. *Limnol. Oceanogr. Lett.* 7, 435–442. doi: 10.1002/lol2.10243

Sarmiento, J. L., Gruber, N., Brzezinski, M. A., and Dunne, J. P. (2004). High-latitude controls of thermocline nutrients and low latitude biological productivity. *Nature* 427, 56–60. doi: 10.1038/nature02127

Sarthou, G., Timmermans, K. R., Blain, S., and Treguer, P. (2005). Growth physiology and fate of diatoms in the ocean: a review. *J. Sea Res.* 53, 25–42. doi: 10.1016/j.seares.2004.01.007

Sathyendranath, S., Stuart, V., Nair, A., Oka, K., Nakane, T., Bouman, H., et al. (2009). Carbon-to-chlorophyll ratio and growth rate of phytoplankton in the sea. *Mar. Ecol. Prog. Ser.* 383, 73–84. doi: 10.3354/meps07998

Schlitzer, R. (2022). *Ocean Data View*. Available at: https://odv.awi.de.

Schmidt, K., and Jónasdóttir, S. (1997). Nutritional quality of two cyanobacteria:How rich is "poor" food? *Mar. Ecol. Prog. Ser.* 151, 1–10. doi: 10.3354/meps151001

Smetacek, V. (2012). Making sense of ocean biota: How evolution and biodiversity of land organisms differ from that of the plankton. *J. Biosci.* 37, 589–607. doi: 10.1007/s12038-012-9240-4

Sommer, U., Stibor, H., Katechakis, A., Sommer, F., and Hansen, T. (2002). "Pelagic food web configurations at different levels of nutrient richness and their implications for the ratio fish production:primary production," in *Sustainable Increase of Marine Harvesting: Fundamental Mechanisms and New Concepts*. Eds. O. Vadstein and Y. Olsen (Dordrecht: Springer Netherlands), 11–20.

Sterner, R. W., Hagemeier, D. D., Smith, W. L., and Smith, R. F. (1993). Phytoplankton nutrient limitation and food quality for Daphnia. *Limnol. Oceanogr.* 38, 857–871. doi: 10.4319/lo.1993.38.4.0857

Tréguer, P., Bowler, C., Moriceau, B., Dutkiewicz, S., Gehlen, M., Aumont, O., et al. (2018). Influence of diatom diversity on the ocean biological carbon pump. *Nat. Geosci.* 11, 27–37. doi: 10.1038/s41561-017-0028-x

Utermöhl, H. (1931). Neue Wege in der quantitativen Erfassung des Plankton. (Mit besonderer Berücksichtigung des Ultraplanktons.): Mit 4 Abbildungen im Text. *SIL Proceedings 1922-2010* 5, 567–596. doi: 10.1080/03680770.1931.11898492